Int. J. Solids Structures, 1967, Vol. 3, pp. 771 to 780. Pergamon Press Ltd. Printed in Great Britain

CIRCUMFERENTIAL AXISYMMETRIC FREE OSCILLATIONS OF THICK HOLLOWED TORI*

DAVID J. MCGILL

School of Engineering Mechanics,
Georgia Institute of Technology, Atlanta, Georgia

and

KENNETH H. LENZEN

Department of Mechanics and Aerospace Engineering,
University of Kansas, Lawrence, Kansas

Abstract—In this article, the effects of thickness and torus radii ratio on the axisymmetric circumferential natural vibrations of freely supported, hollowed tori are determined. The solutions for eigenfrequencies and eigenmodes are effected by finite difference approximations of the basic equations of elastic motion, written in terms of a set of toroidal coordinates. The results agree quite well with the special cases of toroidal membranes and infinite circular cylinders.

1. INTRODUCTION

THE hollowed torus is utilized in many areas of science and engineering, for example, as space vehicle liquid storage containers, and nuclear particle accelerators. The toroidal geometrical shape is also being considered by N.A.S.A., in their design of inflatable manned rotating spacecraft [1]. Thicknesses of tori in most applications are small enough to permit shell theory analyses to be performed; however, it is always of interest to determine the effect of thickness on the vibrations of shells. This has been done extensively for the cylinder [2, 3], by means of the exact equations of linear elasticity.

In this paper, one of the two classes of axisymmetric motion which exist for the torus is examined, using an expansion of the basic equation of elastic motion into toroidal coordinates. The effects of thickness and the radii ratio upon the eigenfrequencies of circumferential free oscillation of the freely supported, hollowed torus is determined, and convergence plots of frequency parameter against fineness of difference mesh are presented as a point of mathematical interest. An excellent check against the solution, contained in [4], for the eigenfrequencies and eigenmodes of axisymmetric circumferential motion of a free toroidal membrane was made by letting the shell thickness in the present analysis become small. Further, the present results reduce to the classical longitudinal free vibrations of an infinite cylinder as the radii ratio approaches zero.

2. PROBLEM FORMULATION

Figure 1 depicts the nondimensionalized geometry of the hollowed torus. The radii R, R_{I}, and R_{II} are respectively equal to the polar coordinate r, the inner radius r_{I}, and the

* This research was sponsored by N.A.S.A. under Project 80-E, Center for Research in Engineering Science, Lawrence, Kansas.

The paper is a revision of the first named author's Ph.D. Thesis, written under the direction of the second author.

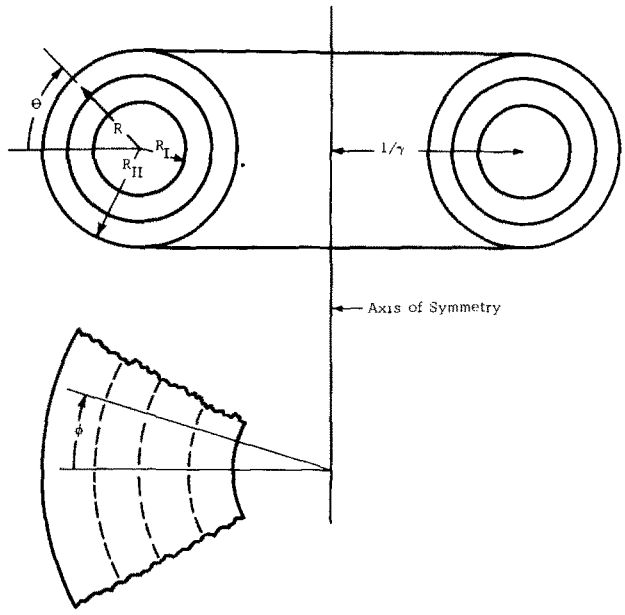

FIG. 1. Nondimensional geometry of the thick toroidal shell.

outer radius r_{II}, all divided by the average radius, $r_0 = (r_I + r_{II})/2$. The torus radii ratio, γ, is taken to be r_0 divided by the distance between the axis of symmetry and the center of any cross-section.

In [5], the basic vector equation of motion of an elastic continuum,

$$(\lambda+2\mu)\nabla(\nabla \cdot \mathbf{u}) - \mu\nabla \times (\nabla \times \mathbf{u}) = \rho\ddot{\mathbf{u}}, \tag{2.1}$$

is expanded into three component equations in toroidal coordinates. In (2.1), $\mathbf{u}$ is the displacement vector, ρ is the density, and λ and μ are Lamé's elastic constants of the isotropic material.

For the case of axisymmetric motion, i.e. motion symmetric with respect to the axis of symmetry of Fig. 1, and hence independent of the circumferential angle ϕ, the governing differential equations and stresses split into two completely independent classes, called the polar and circumferential problems. The polar problem, involving radial (u_r) and tangential (u_θ) displacements in meridional planes, has the three normal stresses, plus the shear in these planes, as its stresses, and there are two governing second order partial differential equations in the two displacements. This problem has been solved [6] by a perturbation technique for the case of a static torus loaded by internal and external pressures. The polar free vibrations of a freely supported, hollowed torus were recently studied by the authors [7]. An early attempt at this problem by Federhofer [8] contains results valid for very thin shells with small radii ratios.

The present paper is concerned with the other, lesser-known class of axisymmetric free vibration of a freely supported torus, involving purely circumferential motion. In this type of vibration, all points move only in the ϕ-direction (Fig. 1) via displacements u_ϕ perpendicular to the meridional planes.

The third of the three partial differential equations, which result upon expansion of (2.1), contains only the circumferential displacement and its derivatives with respect to R and θ in the case of axisymmetry, and may be written as

$$\frac{\partial^2 U_\phi}{\partial R^2}+\frac{1}{R^2}\frac{\partial^2 U_\phi}{\partial \theta^2}+\left[\frac{1+2\gamma R\cos\theta}{R(1+\gamma R\cos\theta)}\right]\frac{\partial U_\phi}{\partial R} -\left[\frac{\gamma\sin\theta}{R(1+\gamma R\cos\theta)}\right]\frac{\partial U_\phi}{\partial\theta}-\left[\frac{\gamma^2}{(1+\gamma R\cos\theta)^2}\right]U_\phi+\Psi^2 U_\phi=0 \tag{2.2}$$

in which

$$\Psi^2=\frac{\rho r_0^2\omega^2}{\mu}.$$

The circumferential displacement u_ϕ has been nondimensionalized, and time eliminated, by the relation

$$u_\phi(r,\theta,t)=r_0 U_\phi(R,\theta)\cos\omega t$$

Here, as usual, ω is the natural circular frequency of free vibration, and t is time.

Of the six possible stresses, only two exist in the present axisymmetric circumferential problem. They are the shears in the r–ϕ and θ–ϕ planes:

$$\sigma_{r\phi}=\left[\frac{-\gamma\mu\cos\theta}{1+\gamma R\cos\theta}\right]U_\phi+\mu\frac{\partial U_\phi}{\partial R} \tag{2.3.1}$$

$$\sigma_{\theta\phi}=\left[\frac{\gamma\mu\sin\theta}{1+\gamma R\cos\theta}\right]U_\phi+\frac{\mu}{R}\frac{\partial U_\phi}{\partial\theta} \tag{2.3.2}$$

The boundary stresses which vanish in general at $R=R_{\mathrm{I}}$ and R_{II} for natural vibrations of hollowed tori with free surfaces are σ_{rr}, $\sigma_{r\theta}$, and $\sigma_{r\phi}$. The axisymmetric boundary conditions are compatible; i.e. in the polar problem there are two second order partial differential equations in two variables (U_r and U_θ) with four boundary conditions (viz. σ_{rr} and $\sigma_{r\theta}$ vanish at $R=R_{\mathrm{I}}$ and R_{II}). In the present circumferential problem there are two boundary conditions ($\sigma_{r\phi}$ vanishes at R_{I} and R_{II}) to go with the second order partial differential equation (2.2) in U_ϕ.

It is noted that equation (2.2) is elliptic and that the circumferential problem posed here is of the mixed boundary value type. Because of the complexity of the governing equation, the solution to the problem is found by finite differences. This solution is carried out in terms of displacements to eliminate the necessity of satisfying compatibility conditions.

3. FINITE DIFFERENCE APPROXIMATIONS AND COMPUTER SOLUTION

In [5] it is proved that all solutions of the exact equations, of which (2.2) is a special case, are such that either

(a) U_r and U_ϕ are even, and U_θ is odd with respect to $\theta=0$ and π, or

(b) U_r and U_ϕ are odd, and U_θ is even with respect to $\theta=0$ and π.

Type (a) will be called symmetric vibrations and type (b), antisymmetric vibrations. Since the above forms comprise all possible solutions, only the upper half of the annulus in the R–θ plane need be considered in drawing the finite difference mesh. When a displacement

at (R, θ) below the rays $\theta = 0$ and π is needed in a difference equation, its coefficient is multiplied by plus or minus the displacement at $(R, 2\pi - \theta)$ within the semiannulus. It should be noted that the signs are dependent upon whether the vibrations are of type (a) or (b).

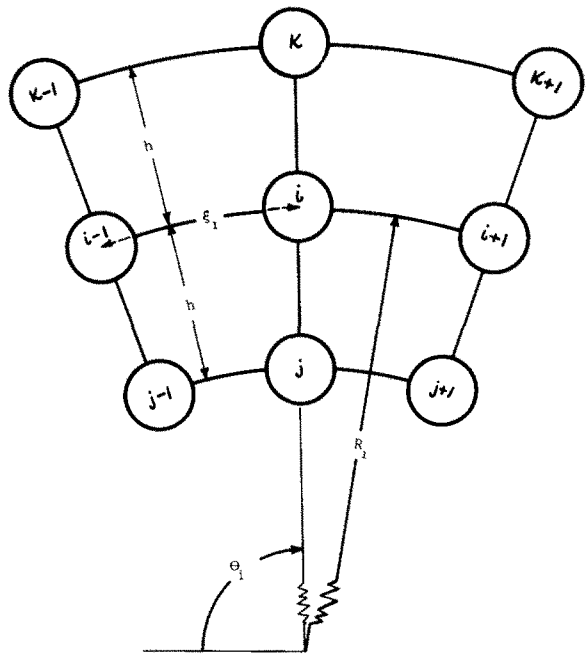

FIG. 2. Mesh point notation.

Simple central difference formulae are used to approximate the derivatives involved in (2.2) and (2.3.1). In the notation of Fig. 2, equation (2.2) becomes

$$\left[\frac{1+2\gamma R_i \cos\theta_i}{R_i(1+\gamma R_i \cos\theta_i)}\right]\left[\frac{U_{\phi k}-U_{\phi j}}{2h}\right]+\left[\frac{U_{\phi k}-2U_{\phi i}+U_{\phi j}}{h^2}\right]-\left[\frac{\gamma^2}{(1+\gamma R_i \cos\theta_i)^2}\right]U_{\phi i}$$
$$+\left[\frac{U_{\phi i+1}-2U_{\phi i}+U_{\phi i-1}}{R_i^2\xi_i^2}\right]-\left[\frac{\gamma \sin\theta_i}{R_i(1+\gamma R_i \cos\theta_i)}\right]\left[\frac{U_{\phi i+1}-U_{\phi i-1}}{2\xi_i}\right]+\Psi^2 U_{\phi i}=0, \tag{3.1}$$

in which h and ξ_i are, respectively, the radial and tangential mesh increments divided by r_0.

When $\sigma_{r\phi}$ from (2.3.1) is written in finite difference form and equated to zero on the free surfaces $R = R_{\mathrm{I}}$ and R_{II}, the difference approximations to the boundary conditions result.

$$\left[\frac{U_{\phi k}-U_{\phi j}}{2h}\right]-\left[\frac{\gamma \cos\theta_i}{1+\gamma R_i \cos\theta_i}\right]U_{\phi i}=0 \qquad \text{at } R_i = R_{\mathrm{I}} \text{ and } R_{\mathrm{II}} \tag{3.2}$$

The difference equation of motion (3.1) is applied to the nodal points on the interior of the region, and also to the boundary nodes, but with modifications. It must be insured that there is no traction on the free surface. Application of (3.1) to the boundary nodes yields fictitious nodal displacements of points lying outside the semiannular cross section.

The values of these displacements (viz. $U_{\phi j}$ on $R = R_{\mathrm{I}}$, and $U_{\phi k}$ on $R = R_{\mathrm{II}}$) are determined from (3.2) in terms of displacements of nodes within and on the boundaries of the cross section. This procedure yields two additional difference equations which are applicable to the boundary nodes.

Computer programs were written which traverse the finite difference mesh, generating the equations of motion at each of the nodes by calculating the non-zero coefficients. These equations form a system which may be written as

$$[A][U]-\Psi^2[U] = 0 \tag{3.3}$$

which constitutes a standard eigenvalue problem. The matrix $[A]$ is the coefficient matrix, and $[U]$ is the column vector containing the circumferential nodal displacements, or the $U_{\phi i}$. To solve the resulting equation $|A-\Psi^2 I| = 0$, the QR Transformation of Francis [9], which is programmed for SHARE by Imad and Van Ness [10], is used.

After the eigenfrequencies Ψ^2 are determined, the mode shapes, or eigenvectors $[U]$, follow easily for any mode number. A node is selected to have a displacement of one unit. Then the corresponding column is shifted to the right side of (3.3), forming a non-homogeneous set of linear algebraic equations. The solution of this system yields the displacement ratios, and it is found by Jordan elimination with no difficulty due to the strength of the principal diagonal of $[A]$.

4. RESULTS OF THE ANALYSIS

The errors involved in the finite difference analysis are known to be of the order of the squares of the mesh increments. Since an exact elasticity approach is used, these difference approximation errors are the only ones that exist. The present method of attack was employed in lieu of a shell approach, in which errors are inherent in the governing differential equations and in which the total error might have been greatly compounded for tori of appreciable thicknesses.

Two very good limiting case checks are available for the out-of-plane modes of this paper. One is the toroidal membrane, which the torus approaches when its thickness goes to zero (i.e. when R_{I} approaches 1). The solution for the free vibrations of a toroidal membrane was obtained by Liepins [4]. One set of modes of his paper dealt with purely circumferential motion. The thickness was taken to be small in order to compare results for the eigenfrequency with those of [4]. For a toroidal shell having $R_{\mathrm{I}} = 0{\cdot}99$, which represents an average radius to thickness ratio of 50, the 24 values of Ψ^2 obtained for various radii ratios and mode numbers differ from the solution based on membrane theory by an average of 1·90%. The mode shapes also show very good agreement when compared to Liepins' curves.

The second limiting case is obtained by letting the radii ratio γ become zero, which results in an infinite cylinder. The solution to purely axial free vibration of such a shell was found by Rayleigh [11] using shell theory. The solution for the eigenfrequency of a torus with $\gamma = 0$ and $R_{\mathrm{I}} = 0{\cdot}99$, executing symmetric vibrations, differs from the classical solution by 0·0, 0·40, 0·97, 1·75, and 2·75% for the first five modes respectively. The classical mode shapes are harmonic in θ, and the present analysis yielded near-perfect cosine $(n\theta)$, $n = 1$–5, curves as the first five mode shapes, for an additional check. Furthermore, a mode with zero frequency was found whenever symmetric modes were examined. Analysis

of the corresponding modal pattern showed that it represented the solution for U_ϕ of $(1+\gamma R\cos\theta)/\gamma$, a rigid body turn of the torus about its axis of symmetry. Since the computer was programmed to yield all solutions for the eigenfrequencies and eigenmodes, this trivial solution was obtained even though it involved no elastic straining, and was an excellent check.

Since the radial mesh increment, h, could be made small by varying the torus thickness, and since the number of equations used to obtain the solution was limited by both computer space and time, three nodes were taken across the thickness in the radial direction. This kept the nondimensional radial and tangential increments approximately the same. It was thought that since the errors inherent in (3.1) and (3.2) are of order h^2 and ξ_i^2, that keeping the increments as nearly equal as possible would yield the best possible difference solution. Several runs were then made with more radial nodes, and for the same number of tangential mesh points, there was indeed very little change in the vibrations.

Convergence plots were then drawn which showed that the eigenfrequencies converged when the tangential mesh increment, ξ_i, became smaller, i.e. when the number of sections formed by the radial lines of the mesh increased. Three of these plots, for the first seven symmetric modes of tori with $R_I = 0{\cdot}9$ and $\gamma = 0, 0{\cdot}3$, and $0{\cdot}75$ are shown in Fig. 3. Figure 4

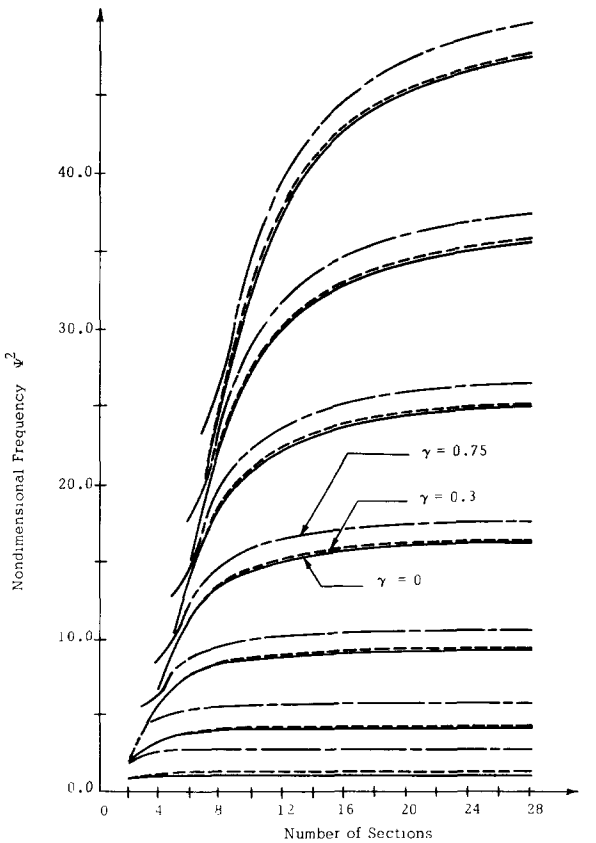

FIG. 3. Convergence plot for circumferential symmetric free vibration of tori with $R_I = 0{\cdot}9$ and $\gamma = 0$, $0{\cdot}3$, and $0{\cdot}75$.

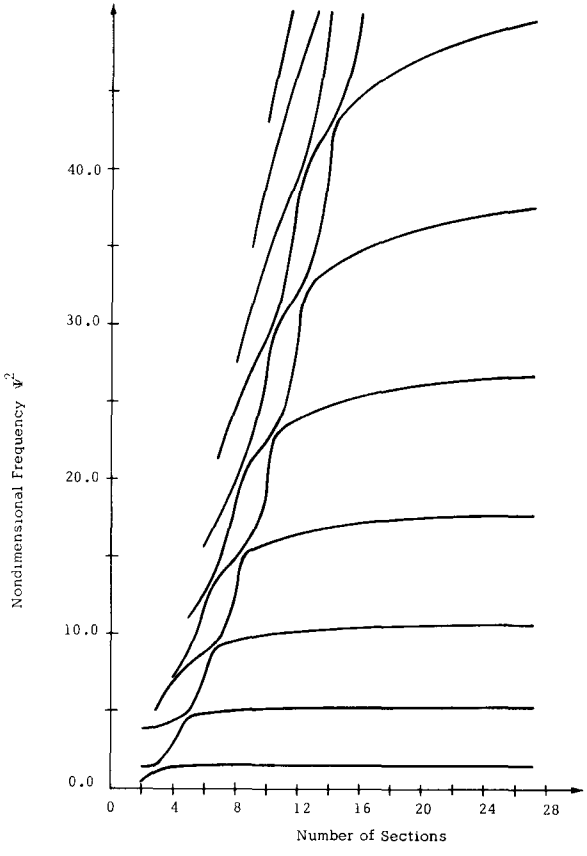

FIG. 4. Convergence plot for circumferential antisymmetric free vibration of a torus with $R_I = 0{\cdot}9$ and $\gamma = 0{\cdot}75$.

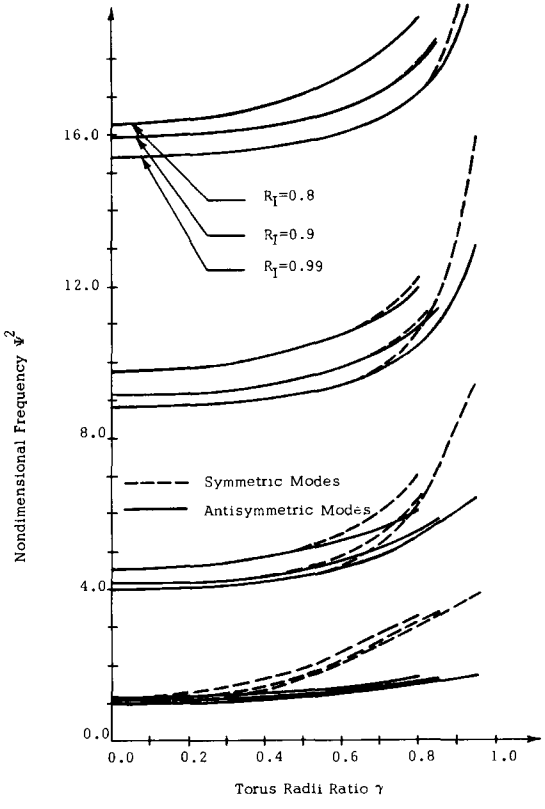

FIG. 5. Frequency parameter vs. torus radii ratio for three thicknesses.

depicts a convergence plot of the seven lowest antisymmetric modes of a torus having $R_I = 0{\cdot}9$ and $\gamma = 0{\cdot}75$. From these curves and other convergence plots, it was seen that 18 or more sections gave a sufficiently fine difference mesh for examination of the effects of other parameters upon the eigenfrequencies and eigenmodes of the lower free vibratory patterns.

Figure 5 shows the first four eigenfrequencies plotted as a function of the torus radii ratio γ for $R_I = 0{\cdot}8$, $0{\cdot}9$, and $0{\cdot}99$. It is seen that there is a considerable increase in frequency as γ increases from zero to its maximum value (which is given in general by $1/(2-R_I)$), which appears for all three thicknesses* considered. It is noted that the antisymmetric and symmetric modes become more and more distinct as the torus deviates more and more from the cylinder, i.e. as γ gets farther from zero. This shows a definite effect of the circumferential curvature on the vibratory modes. The symmetric frequencies are higher than the antisymmetric ones, indicating that it is easier for sections to shear past each other in horizontal than in vertical planes.

Figure 6 shows the effect of thickness on the eigenfrequencies of the first three modes for both symmetric and antisymmetric modes, and for three values of γ. It is seen that frequency increases with thickness. This is because a thicker shell is stiffer, requiring a higher frequency to vibrate it in a given nodal pattern.

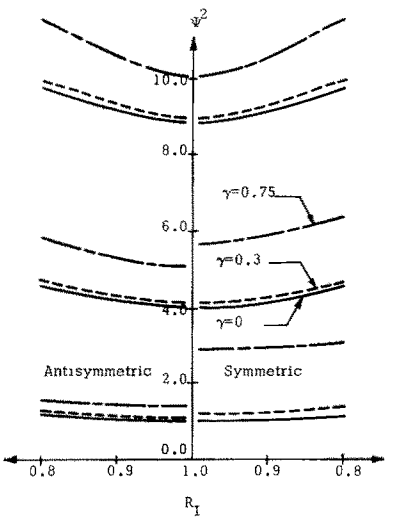

FIG. 6. Frequency parameter vs. nondimensionalized inner radius for symmetric and antisymmetric modes, and for three values of γ.

The first four mode shapes of the middle surface nodes of symmetric circumferential vibration of a toroidal shell with $\gamma = 0{\cdot}75$ and $R_I = 0{\cdot}99$ are shown in Fig. 7. The corresponding curves for a cylindrical shell are cosine $(n\theta)$, $n = 1$–4 (which were obtained with $\gamma = 0$), hence, the distortion caused by a considerable amount of circumferential curvature can be seen.

* The nondimensional thickness is $2(1-R_I)$, so that as R_I approaches 1, the thickness approaches zero. The inner radii $R_I = 0{\cdot}8$, $0{\cdot}9$, and $0{\cdot}99$, therefore, correspond to average radius to thickness ratios of 2·5, 5, and 50, respectively.

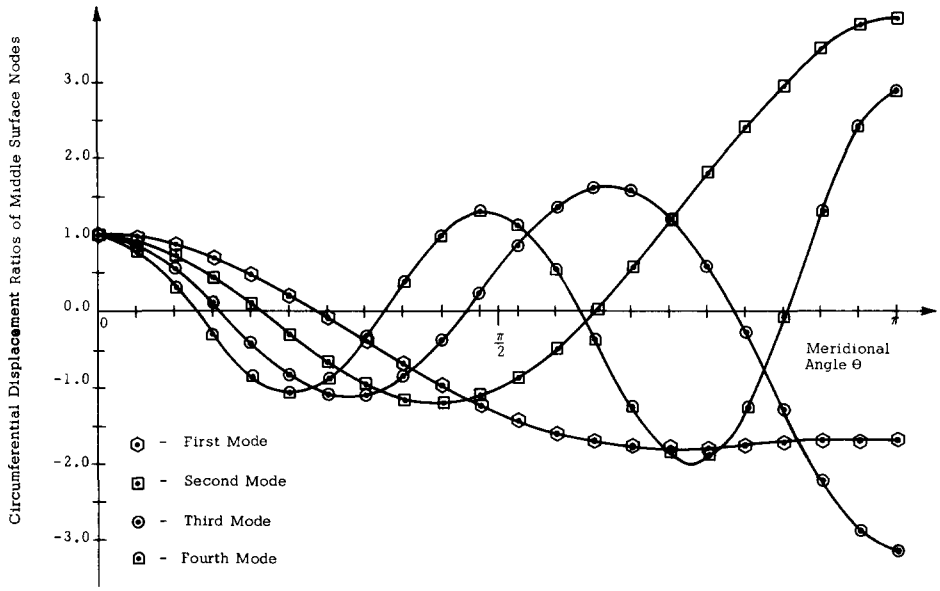

FIG. 7. The first four circumferential symmetric free vibratory modes of a toroidal shell with $R_1 = 0{\cdot}99$ and $\gamma = 0{\cdot}75$.

The modal frequencies of polar motion [7] are dependent upon Poisson's ratio ν, whereas the present circumferential vibrations are dilatationless, and independent of ν. Both classes of vibration occur at high frequencies. For $\nu = 0{\cdot}3$, the polar circular frequencies of [7] were compared with the present circumferential circular frequencies for several thicknesses, and the two were seen to be interspersed, and of the same order of magnitude for the lower modes examined.

Another result, discussed in more detail in [5], is that the present elasticity theory demonstrates that at any angle θ, the node across the thickness at which the magnitude of the Gaussian curvature is smallest tends to have the largest displacement. This is because the Gaussian curvature is a measure of the net amount of curvature at a point, and curvature is known to stiffen a shell.

REFERENCES

[1] A report containing 12 articles by a total of 24 authors. "A Report on the Research and Technological Problems of Manned Rotating Spacecraft", Langley Research Center Staff, Langley Research Center. *N.A.S.A.* TN D-1504 (Aug. 1962).

[2] D. C. GAZIS, Exact analysis of the plane-strain vibrations of thick-walled hollow cylinders. *J. acoust. Soc. Am.* **30**, 786 (1958).

[3] D. C. GAZIS, Three-dimensional investigation of the propagation of waves in hollow circular cylinders. *J. acoust. Soc. Am.* **31**, 568 (1959).

[4] A. A. LIEPINS, Free vibrations of the prestressed toroidal membrane. *A.I.A.A.* Paper No. 65-110 (Jan. 1965).

[5] D. J. MCGILL, Axisymmetric free oscillations of thick toroidal shells. Ph.D. Thesis, University of Kansas (June 1966).

[6] A. KORNECKI, Stress distribution in a pressurized thick walled toroidal shell—a three dimensional analysis. *College of Aeronautics* (*Cranfield*) Note 137 (Jan. 1963).

[7] D. J. MCGILL and K. H. LENZEN, Polar axisymmetric free oscillations of thick hollowed tori. To be published in the *SIAM Jnl.*

[8] K. FEDERHOFER, Zur Schwingzahlberechnung des dunnwandigen Hohlenreifens. *Ing.-Arch.* 10–11, pp. 125–132 (1939–40).
[9] J. G. F. FRANCIS, The *QR* transformation—a unitary analogue to the *LR* transformation. *Comput. J.* **4**, 265–271, 332–345 (1961).
[10] F. P. IMAD and J. E. VAN NESS, Eigenvalues by the *QR* transform. *SHARE* Program Catalog, Program Description Submittal SDA No. 3006–01 (Aug. 1964).
[11] LORD RAYLEIGH, *The Theory of Sound*, volume 1, 2nd edition, pp. 402–409. Dover (1945).

(*Received* 27 *October* 1966; *revised* 26 *January* 1967)

Résumé—Dans cet article, les effets du rapport de l'épaisseur au rayon du tore sur les vibrations naturelles circonférentielles symétriques selon l'axe de tores creux, supportés librement sont déterminés. Les solutions pour fréquences propres et modes propres sont obtenues par des approximations à différence finie des équations de base du mouvement élastique, posées d'après un ensemble de coordonnées toroïdales. Les résultats s'accordent très bien avec les cas spéciaux des membranes toroïdales et des cylindres circulaires infinis.

Zusammenfassung—In dieser Arbeit wir der Einfluss von Dicke und und Ringhalbmesserverhältnis auf die axialsymmetrischen natürlichen Umfangsschwingungen eines frei gestützten Torusringes bestimmt. Die Lösungen der Eigenfrequenzen und Eigensysteme werden durch begrenzte Differenz-Annäherungen der Grundgleichung für elastische Bewegung bestimmt, die in Toroidalkoordinaten ausgedrückt sind. Die Resultate zeigen gute Übereinstimmung mit den Spezialfällen für Toroidalmembranen und für unendliche kreisförmige Zylinder.

Абстракт—В этой статие выведены эффекты отношения толщины и радиуса торуса на поведение осесимметричных, кольцевых, натурных колебаний в свободно опертых, полых торусах. Решения для собственных частот колебаний и собственных форм колебаний осуществляется с помощью конечно разностного приближения основных уравнений упругого движения, описанного в виде системы тороидальных координат. Результаты почти согласовываются со специальными случаями тороидальных мембран и бесконечных круглых цилиндров.